European Journal of Molecular & Clinical Medicine
ISSN 2515-8260 Volume 7, Issue 06, 2020

The Effect Of Doxorubicin Loaded Silica Nanoparticles On The Expression Of PARP-1 In Head And Neck Squamous Carcinoma Cell Line: In Vitro Study.

Nihal Mohamed Darwish; Heba Mahmoud Dahmoush and Safa Fathy Abd El- Ghany

Faculty of Dentistry, Cairo University, Egypt

ABSTRACT:Nanotechnology is a new branch of science, which is going to be a major driving force behind the impending technological revolution in the 21st century. Although Doxorubicin (DOX) is one of the preferred chemotherapeutic drugs for the treatment of oral squamous cell carcinoma (OSCC), several studies pointed out that it was limited due to multidrug resistance (MDR) like the over-expression of DNA damage repair agents as poly (ADP-ribose) polymerase-1 (PARP-1). Accordingly, it seemed very interesting to explore the effect of DOX loaded mesoporous silica nanoparticles (MSNs) with their outstanding properties in comparison to the conventional DOX on HNO-97 cell line, in an attempt to introduce a novel efficient therapeutic modality for OSCC.

INTRODUCTION:

Nanotechnology is a new branch of science, which is going to be a major driving force behind the impending technological revolution in the 21st century. The potential of this technology is so great that the governments of the most developed nations have promoted investments in this field for the past 20 years. Nanotechnology has many fields to be explored especially in medicine, it can offer new concepts and approaches including nano diagnostics, cancer chemotherapy, photo thermal antimicrobial nano therapy, newer drug delivery systems, nano robots, cell repair and many more which allow better and earlier diagnosis of the patients as well as treating them with the least possible interventions and adverse effects. In future, we expect that nanomaterials will be our daily companions not only in hospitals but also in our homes. In addition, it will provide smarter products for communications, transportation, agriculture and industry(Tevatia et al., 2016). Cancer is a critical public health problem worldwide that has brought great burden to society. Oral cancer is an aggressive cancer that accounts for approximately 3% of all malignancies. Most of the oral cancers occur as squamous cell carcinoma (SCC) which may commonly develop metastases and results in death. Despite remarkable advances in treatment modalities, the 5-year survival rate has not significantly improved over the past several decades and still hovers around 40-50% (Zhao et al., 2020).

At present, chemotherapy is one of the most effective non-invasive treatments; The US Food and Drug Administration (FDA) has approved many anticancer drugs. Doxorubicin (DOX) is a member of the anthra-cycline family that exhibits a broad spectrum of antitumor activity and a great therapeutic effect against a number of malignancies. However, a growing body of evidence supported the view that DOX could be a double-edge sword, which reduces tumor activity efficiently but unfortunately causes injury to non-targeted tissues. Indeed, this injury often complicates cancer treatment by limiting therapeutic dosages of DOX and diminishing the quality of patients' life during and after treatment. Several studies showed that the heart is a preferential target of DOX toxicity but it also affects other organs like the brain, kidney and liver (Fang et al., 2019).

On the other hand, several studies pointed out that treating OSCC patients with conventional DOX has been limited due to multidrug resistance (MDR). MDR is a term used to describe the phenomenon

characterized by the ability of tumor cells to exhibit simultaneous resistance to a number of chemotherapeutic drugs and the over-expression of drug efflux agents as poly (ADP-ribose) polymerase-1 (PARP-1) which is considered one of the main reasons of MDR in cancer cells (Ye et al., 2019).

PARP-1, a nuclear protein enzyme, is considered as a key sensor of DNA damage. It stands at the beginning of the DNA repair cascade, and its activation causes recruitment of other DNA repair factors. Its overexpression has been reported in a wide variety of cancers. Recently, PARP-1 expression has been used to identify tumor cells from surrounding healthy tissues and to test the efficacy of chemotherapeutic treatment (Kossatz et al., 2016). Furthermore, its inhibition could be a possible pathway for effective cancer treatment that not only enhances the anticancer effect of chemotherapeutic drugs but also overcomes resistance against them (Kossatz et al., 2019).

The rising of nanotechnology has provided a versatile platform for cancer treatment because of their large surface-to-volume ratio, high flexibility for surface tailoring, and excellent capacity for multifunction. Nanoparticles (NPs) have recently emerged as a promising carrier for co-delivery of DOX to evade MDR where they bypass the efflux PARP-1, increase drug accumulation in cancer cells, improve drug solubility and reduce systemic toxicity (Liu et al., 2106). However, theses NPs suffer from many biochemical attacks in vivo due to their instability so, it has become a significant challenge to develop a safe and efficient drug delivery system to overcome DOX efflux and reverse MDR (Chen et al., 2018).

2. MATERIALS AND METHOD

The cell line, drug and nanoparticle were all purchased from Nawah scientific Inc. where the experiment was performed in their labs.

Study Design

First, DOX was loaded on MSNs then the encapsulation efficiency percentage was determined to ensure proper loading of the drug on NPs prior to the experimental procedures. Then, we sub-cultured HNO-97 cell line to obtain three study groups: **DOX group** where the cell line was subjected to DOX only, **DOX/MSNsgroup** where the cell line was subjected to DOX loaded on silica NPs and the rest of the cell line was used without any addition as a **normal control group**. After incubation for 72 hours, morphological assessment of all the three groups was done at 25μg/ml and 100 μg/ml drug concentration using inverted phase contrast microscope. The cells were then tested for viability and toxicity using MTT assay. The percentage of apoptosis was determined by measuring the expression of caspase-3 using flow cytometry. On the other hand, MDR was determined by expression of PARP-1 using ELISA. The study design is summarized in Table (1):

Preparation of DOX loaded MSNs:

50 mg MSNs were added to a water solution containing DOX (2.5 ml, 10mg/ml), and then the mixture was ultra-sonicated for 5 minutes, followed by stirring for 24 hours to allow the drug to enter the MSN framework

The solution was centrifuged, washed and dried at 50 ºC for 24 hours.

Table (1): Summary of the study design

Drug used	DOX		
Nanoparticles used	MSNs		
DOX loaded on MSNs	Measurement of loading capacity and encapsulation efficiency		
Cell line used	HNO-97		
Study groups	DOX	DOX/MSNs	Control
The used IC50 dose of DOX	0.75±0.04	0.47±0.03	No drugs
Parameters Assessed	Morphological analysis using inverted phase contrast microscope at 100µg/ml drug concentration		
	Cell viability and cytotoxicity using MTT assay		
	Caspase-3 expression using flow cytometry		
	Expression of PARP-1 using ELISA		

Determination of the encapsulation efficiency and loading efficiency:

- The DOX loaded MSNs were centrifuged and washed with 20 mL of PBS (pH 7.4).
- The supernatant was collected, this step was repeated several times then the residual DOX content (RDOX, mg) was determined (5.4 mg)**.**
- The DOX loading capacity (LC) reflect the mass ratio of drugs to nano medicines and is determined by the structure, physical and chemical properties of the carrier material which was calculated as follows:

Q = (10 - RDOX)/0.005 (mg/g)

(10: is the weight of DOX (mg) and 0.005 is the weight of Silica added).

- The DOX encapsulation efficiency percentage (EE %) is the percentage of DOX that is successfully entrapped into MSNs and it reflects the utilization of drugs in feed during the nanomedicine-preparation process. It is determined by the drug loading mechanism which was calculated as follows:

$$\boldsymbol{EE\ percentage} = \frac{\boldsymbol{Total\ DOX\ added - RDOX}}{\boldsymbol{Total\ DOX\ added}} \times \boldsymbol{100}$$ (Thashini et al., 2020).

Morphological assessment using inverted phase microscope:

For microscopy imaging, HNO-97 cell lines were seeded in 6-well plate and grown overnight at 37°C. For the DOX and the DOX/MSNs cell line groups, the medium was replaced with a fresh medium containing 100µg/ml of the drug formulations and incubated for 72 h.

Measuring cell viability using MTT assay:

The cultures were removed from incubator into laminar flow hood. DOX and DOX/MSNs were added to cell lines with serial dilutions (100µg/ml, 25µg/ml, 6.25µg/ml, 1.56µg/ml and 0.39µg/ml. Then 20µL of MTT reagent was added to each well and left in incubator for four hours at 37ºc until intracellular purple formazan crystals were visible under inverted microscope. The percentage of cell viability was calculated by dividing the absorbance reading from the test samples by that of the control and multiplied by 100

$$Viability\ percentage = \frac{sample\ absorbance - blank\ absorbance}{control\ absorbance - blank\ absorbance} \times 100.$$

Finally, a graph was plotted between the log concentrations on the X-axis versus percentage of viability on the Y-axis (Table 2). The equation mx=C was used, as m and C were constants, Y substituted by 50 and hence the x value was calculated. The x value was the IC50 value. A curve was plotted between them for each study as shown below (Fig 1).

Table (2): Log concentration and mean viability percent of (A): DOX and (B): DOX/MSNs

A	
Log conc.	**% Viability**
2	**16.2636**
1.39794	**29.7461**
0.79588	**38.3918**
0.19312	**45.2237**
-0.40894	**52.7811**
IC50=0.75±0.04	

B	
Log conc.	**% Viability**
2	**11.7896**
1.39794	**24.24426**
0.79588	**33.01088**
0.19312	**42.20073**
-0.40894	**50.42322**
IC50=0.47±0.03	

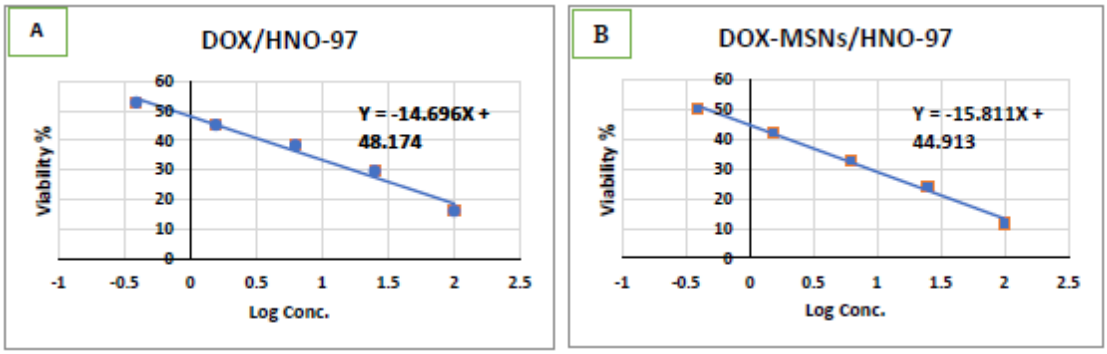

Fig (1): Graphs showing relation between log concentration of (A): DOX and (B): DOX-MSNs and the viability percentage of HNO-97.

Protocol of caspase-3 FITC flow cytometry:

1. Perm/Wash™ buffer (10X) 1:10 was diluted in distilled water prior to use.
2. The cells were washed twice with cold 1X PBS, then suspended in Cytofix solution at a concentration of 1x10^6 cells/0.5 ml.
3. Then they were incubated for 20 min on ice.
4. Cells were formed into pellets and Cytofix buffer was aspirated and discarded then the cells were washed twice with Perm/Wash™ buffer (1X) at a volume of 0.5 ml buffer/1x10e6 cells at room temperature.
5. After that, cells were suspended in the Perm/Wash™ buffer (1X) plus antibody and incubated for 30 min at room temperature.
6. Finally, they were washed again in 1.0 ml Perm/Wash™ buffer (1X) and suspended in 0.5 ml Perm/Wash™ buffer (1X) to be analyzed by flow cytometry.
7. Analysis was performed using ROBONIK p2000 ELISA reader, with data displayed as frequency histograms.
8. All previous steps were repeated 3 times and average was calculated.

ELISA preparation protocol

PARP-1 reagent was equilibrated to ambient room temperature prior to use in the procedure.

1. 100 µL of serially titrated standards were added into wells of the PARP1 Microplate.
2. The plate was covered with the well plate lid and incubated at 37°C for 2 hours.

3. One hundred µL of prepared **1X Biotinylated PARP1 Detector Antibody** was addedto the well. Then, the well-plate lid was put and incubated at 37°C for 60 minute
4. After that, the plate was washed 3 times with **1X Wash Buffer.**
5. The previous steps were repeated twomore times. Then, 100 µL of prepared **1X Avidin-HRP Conjugate** was added into the well and incubated at 37°C for 60 minutes.
6. The plate was washed **5 times** with **1X Wash Buffer,** then90 µL of **TMB Substrate** was added and incubated at 37°C in the dark for 15 minutes.
7. Finally, 50 µL of the Stop **Solution was added** for 5 minutes then the optimal density (OD) was read at 450 nm with a standard microplate reader and a curve was obtained as shown in Fig (2).
8. The experiment was repeated three times and average was calculated

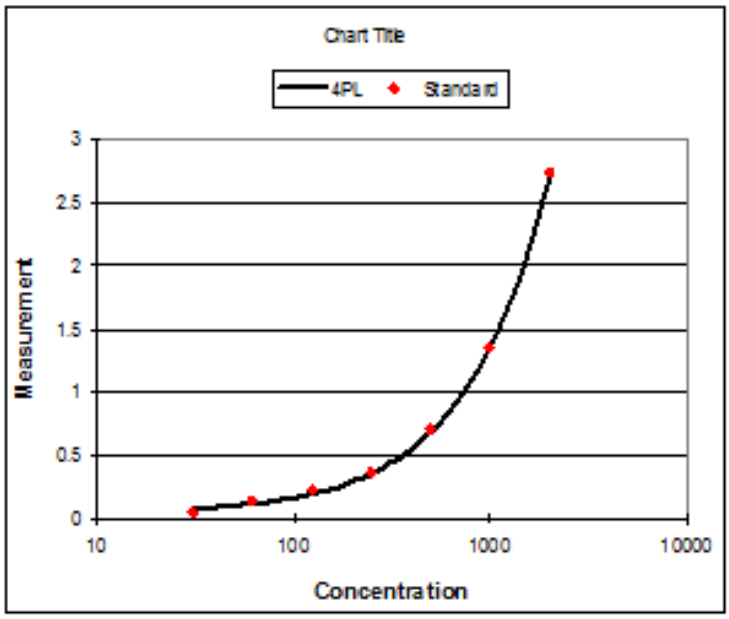

Fig (2): A standardized curve for ELISA reader.

Statistical methods

Data were coded and entered using the statistical package SPSS version 26 (IBM Corp., Armonk, NY, USA). They were summarized using mean and standard deviation for quantitative variables. Comparisons between groups (Control, DOX and DOX/MSNs) were done using analysis of variance (ANOVA) with multiple comparisons post hoc Tukey test for comparison between two groups was done. P-values ≤ 0.05 will considered as statistically significant. The P value was considered as follows:

- P value ≥ 0.05, not significant
- P value ≤ 0.05, significant
- P value ≤ 0.001, highly significant

RESULTS

3.1. Assessment of encapsulation efficiency and loading capacity:

The loading capacity (LC) of DOX was found to be **938.43 ±14.3 mg/g** while DOX encapsulation efficiency (EE %) was **46±1 %.** Our investigation revealed a linear relation between concentration of DOX used and the amount absorbed into MSNs which is represented in the following fig (3).

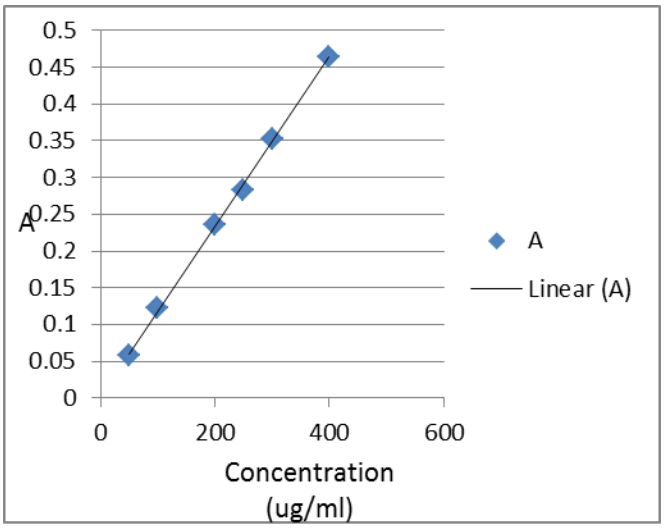

Fig (3): Graph showing relation between DOX concentration and amount of absorbance into MSNs

Morphological analysis

The morphological analysis of viable cells in the 3 experimental groups showed marked decrease in cell population of both DOX and DOX/MSNs groups in comparison to the control group. However, reduction in viable cells was more obvious in the Dox/MSNs group. In addition, in the control group, the viable cells appeared to be polygonal and maintained intercellular attachments. On the contrary, round and detached viable cells in both groups DOX and DOX/MSNs were observed (Fig 4).

Assessment of toxicity and cell viability using MTT assay:

In the MTT assay, solubilization of formazan crystals resulted in a colored solution which appeared purple in the control group. On the other hand, the solution showed very faint purple color in the DOX and DOX/MSNs groups (Fig 5). Results showed reduction in the viable cells in both DOX and DOX/MSNs groups, which was inversely proportional to drug concentration increase. However, the percentage of viable cells was lower in the DOX/MSNs group than in the DOX group (Table 3) (Fig 6). Post hoc pair wise comparisons showed a significant difference between DOX and DOX/MSNs groups at concentrations 0.39 µg/ml, 6.25 µg/ml and 25 µg/ml. On the contrary, the other 2 concentrations (1.56 µg/ml and 100 µg/ml) showed insignificant differences (Table 4).

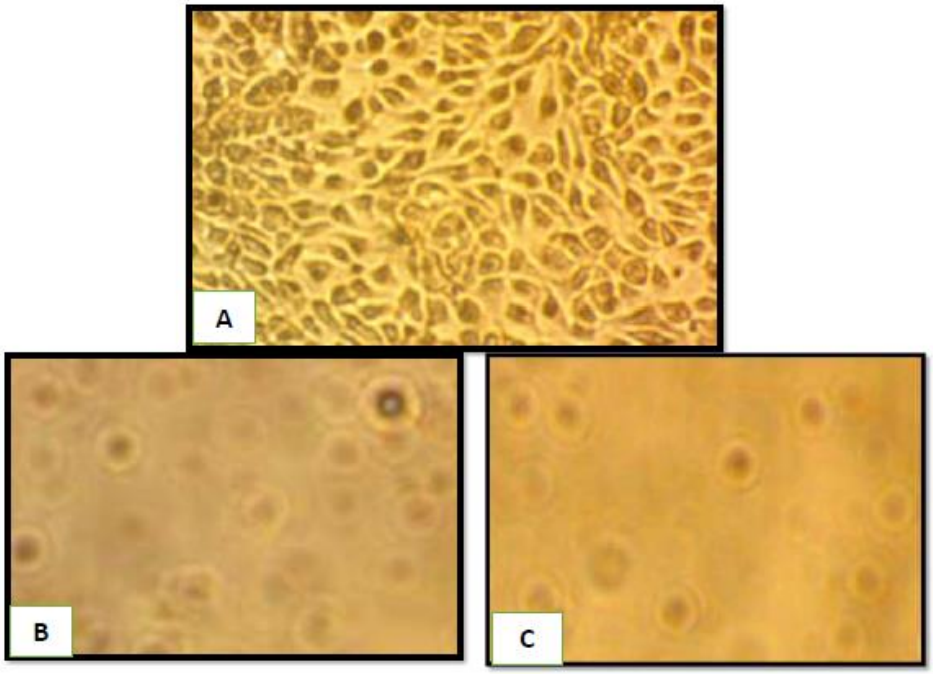

Fig (4): Photomicrographs showing viable cells of HNO-97 cell line in: (A) control group, (B) DOX group, (C) DOX/MSNs group at 100µg/ml conc.

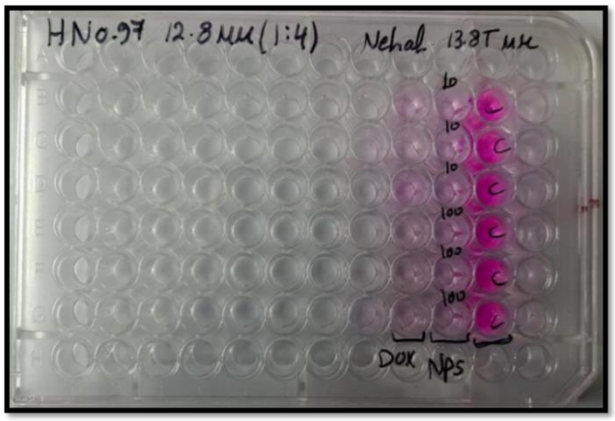

Fig (5): A photo showing color of MTT in the control, DOX and DOX/MSNs

Table (3): Raw data showing percentage of cell viability at different concentrations of DOX and DOX/MSNs

DOX					DOX-MSNs				
0.39ug/ ml	1.56ug/ ml	6.25ug /ml	25ug/ ml	100ug/ ml	0.39ug/ ml	1.56ug/ ml	6.25ug/ ml	25ug/ ml	100ug/ ml
54.17	47.12	38.03	29.13	19.29	51.58	42.86	33.77	25.60	11.87
53.43	44.77	38.09	29.96	14.26	50.72	41.16	31.59	22.02	13.00
54.36	43.85	39.04	30.12	15.33	49.02	42.60	33.69	25.13	10.52

Table (4): Mean and SD of cell viability among the experimental groups

	DOX	DOX/MSNs	P value
	Mean ± Standard Deviation	Mean ± Standard Deviation	
0.39ug/ml	53.99 ± 0.49	50.44 ± 1.3	0.012*
1.56ug/ml	45.25 ± 1.69	42.21 ± 0.92	0.052
6.25ug/ml	38.39 ± 0.57	33.02 ± 1.24	0.002*
25ug/ml	29.74 ± 0.53	24.25 ± 1.95	0.009*
100ug/ml	16.29 ± 2.65	11.8 ± 1.24	0.056

*Significant

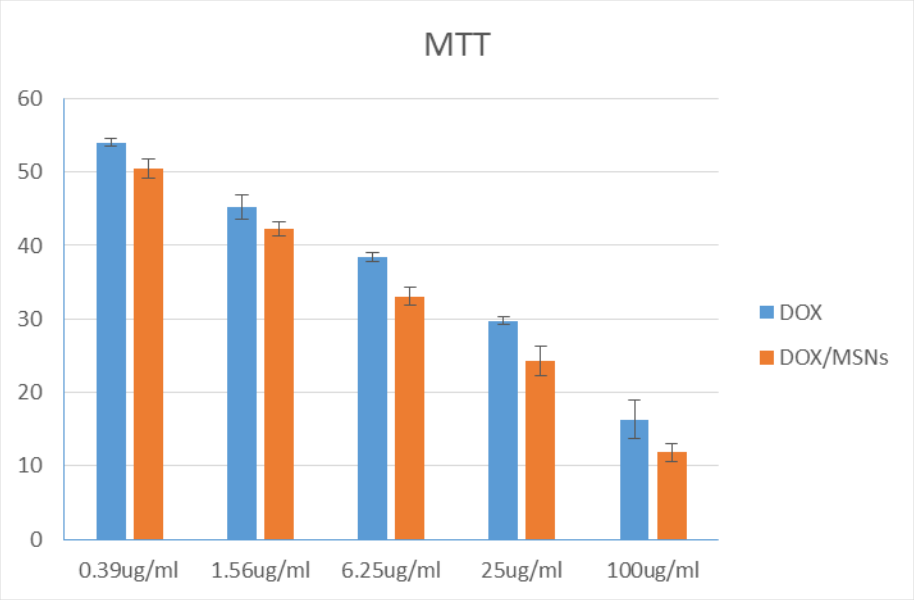

Fig (6): Column chart representing the percentage of cell viability of HNO-97 at various concentrations of DOX and DOX/MS in the experimental groups.

Expression of caspase-3 using flow cytometry

Flow cytometry revealed that the highest levels of expression of caspase-3 were detected in DOX/MSNs, followed by the DOX group. On the other hand, the control group showed the lowest value of caspase-3 expression (Fig 7). ANOVA analysis among the three experimental groups showed highly significant statistical difference in levels of caspase-3 expression with a P value < 0.001 (Table 5).All the post hoc pair wise comparisons showed high statistically significant differences on comparing each two groups together (Table 6).

Table (5): ANOVA analysis of caspase-3 expression levels among the experimental groups

	Control	DOX	DOX/MSNs	P value
	Mean ± Standard Deviation	Mean ± Standard Deviation	Mean ± Standard Deviation	
Caspase-3	2.20 ± 0.02	23.64 ± 0.38	32.12 ± 0.02	< 0.001**

** Highly Significant

Table (6): Post hoc pair wise comparisons of caspase-3 expression levels among the experimental groups

		Control	DOX	DOX/MSNs
Caspase-3 %	Control	----------	< 0.001**	< 0.001**
	DOX	< 0.001**	----------	< 0.001**
	DOX/MSNs	< 0.001**	< 0.001**	----------

** Highly significant

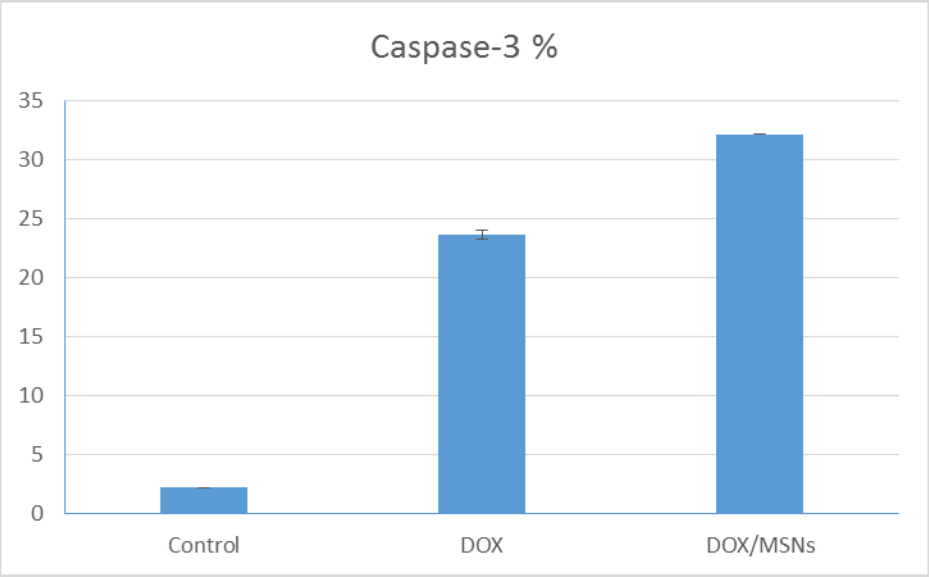

Fig (6): Column chart showing expression of caspase-3 among the experimental groups

Assessment of PARP-1 expression by ELISA

ELISA results showed that the highest levels of PARP-1 expression was obtained in the DOX group, followed by DOX/MSNs group. The lowest levels were detected in the control group (Fig 7). ANOVA test among the three experimental groups showed high statistically significant difference in PARP-1 expression levels with a P value < 0.001 (Table 7). On the other hand, all the post hoc pair wise comparisons showed high statistically significant difference with P values < 0.001 (Table 8).

Table (7): ANOVA analysis of PARP-1 expression among the experimental groups

	Control	DOX	DOX/MSNs	P value
	Mean ± Standard Deviation	Mean ± Standard Deviation	Mean ± Standard Deviation	
PARP-1	179.53 ± 4.79	387.53 ± 9.45	275.90 ± 7.18	< 0.001**

** Highly significant

Table (8): Post hoc pair wise comparisons among the experimental groups

		Control	DOX	DOX/MSNs
PARP-1	Control	----------	< 0.001**	< 0.001**
	DOX	< 0.001**	----------	< 0.001**
	DOX/MSNs	< 0.001**	< 0.001**	----------

** Highly significant

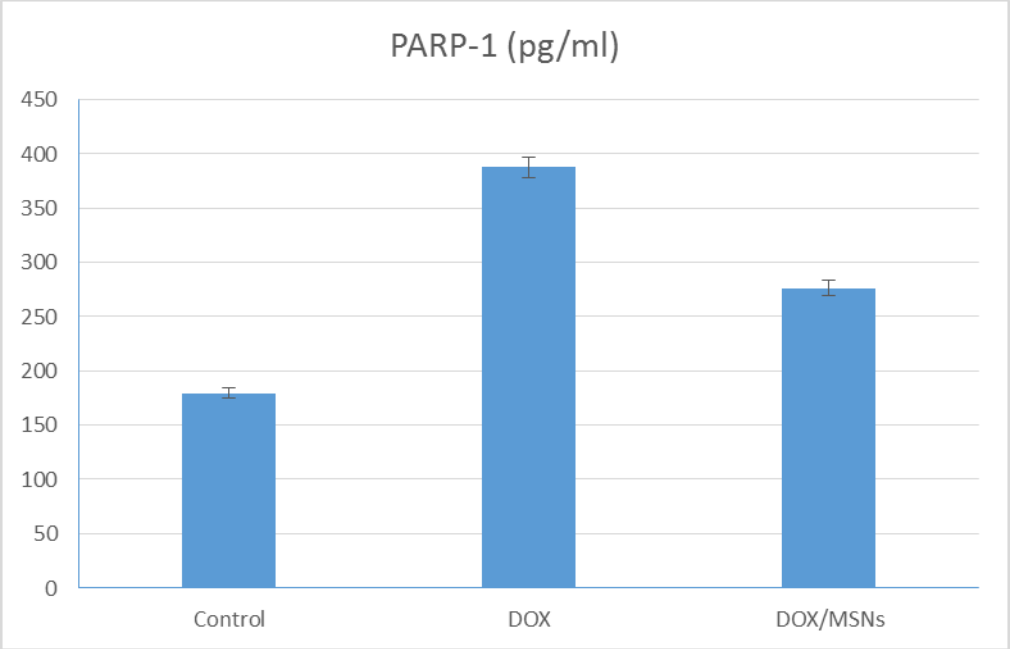

Fig (7): Column bar chart showing levels of PARP-1 expression among the experimental groups

DISCUSSION

Our study pointed out that DOX encapsulation efficiency increased with increasing amounts of DOX input. In addition, our loading technique achieved our goal of acceptable loading capacity and encapsulation efficiency for regulation of DOX release at the cancer site and in the same time preventing crystallization of the drug in HNO-97 cell line. In accordance with our findings, the studies of Geng et al. (2016) and Huang et al. (2018) reported values of drug loading capacity and encapsulation efficiency that were very close to ours. Cytotoxicity is one of the most important indicators for biological evaluation in in-vitro studies. In our study, we used MTT assay, which is considered the gold standard of cytotoxicity assays due to its high sensitivity. Determination of the IC50 values shows that DOX/MSNs have induced effective cytotoxicity of OSCC cells using only half the dose of DOX alone. This could be attributed to the ability of the DOX loaded NPs to enter the cancer cells easily. Reduction in the dose of such a chemotherapeutic drug will possibly reduce the associated unfavorable side effects in OSCC patients.

In the present work, although both DOX and DOX/MSNs showed dose dependent reduction in cell viability of HNO-97 cell line, the superior results of DOX/MSNs suggest a more potentcytotoxic anticancer effect. This effect could be attributed to multiple mechanismsincluding generation of ROS, inducing DNA damage through inhibition of type II topoisomerases,that inhibit DNA and RNA synthesis. In addition, the ability of DOX to inhibit the PI3K/Akt pathway, which plays an important role in activating Hg signaling proteins that are responsible for cancer cell proliferation, migration and metastasis, was also reported (Smolensky et al., 2017).

Regarding caspase-3 expression among the studied groups, DOX/MSNs revealed the highest level of caspase-3 expression followed by the DOX group, which suggests that DOX anticancer potential activity might be linked to the induction of apoptosis though activation of the caspase-3 execution pathway. Moreover, loading to NPs has enhanced the ability of DOX to induce apoptosis and offered superior results. In agreement with our study, Geng et al. (2016) and Kim et al. (2018) stated that caspase-3 expression increased in DOX/NPs in a dose dependent manner and that multidrug loading on NPs induced more apoptotic effect.

Cell morphology of HNO-97 cell line was assessed among the experimental groups, as it is an important aspect that reflects regulation of cell activities and general condition of a cell. Cancer cells in both DOX and DOX/MSNs groups lost the polyhedral shape which was seen in the control group and attained a more rounded outline, this could be attributed to reduction in cell population and subsequent loss of intercellular adhesion mechanisms and loss of polarity, as well. In addition, enlargement of the cells with condensation of the cytoplasmic content was also noted and may indicate beginning of some changes in cancer cells as preparatory steps, which finally will lead to apoptosis. Ibiyeye et al. (2019) reported similar findings.

MDR is one of the major obstacles for successful chemotherapy in cancer. One the mechanisms that cancer cells use in MDR is increasing repair of DNA damaged by chemotherapeutic drugs by expressing the DNA repair enzyme PARP-1. Most of the previous studies paid more attention to reverse the MDR after it has already occurred which was far in adequate in clinical trials. We thought it might be more effective to delay or prevent the MDR resistance in the initial chemotherapeutic drug. One of the effective approaches to achieve this to use nanoparticle-mediated drug delivery to increase drug accumulation in drug resistant cancer cells. In our study we identified the expression of PARP-1 in DOX and DOX/MSNs to determine whether this combination was able to overcome drug resistance. Thus, this will provide a more efficient and less toxic possible treatment for such a common malignancy.

Interestingly, we detected the highest levels of PARP-1 in the DOX group; this may be attributed to development of DOX-resistant cancer cells, where accumulation of DNA damage took place and so elevated PARP-1 levels. This finding is consistent with results of Liu et al. (2016) who noted that PARP-1 expression in head and neck SCC cell line significantly increased after treatment with DOX due to resistance of cancer cells. Moreover, Du et al. (2017) attributed the development of DOX-resistant OSCC cells to upregulation of miR-221 which has downregulated tissue inhibitor of metalloproteinase-3 (TIMP3); they added that inhibition of miR-221 with anti-miR-221 has increased the sensitivity of OSCC cells to DOX and succeeded in decreasing cancer cell viability.

On the contrary, lower levels of PARP-1 in the control group reflects that the amount of damaged DNA in cancer cells was low. The lowest levels detected in DOX/MSNs group highlights the ability of DOX/MSNs in reducing PARP-1 expression, decreasing DNA damage repair and finally reversing MDR and induce apoptosis. Liu et al. (2016) obtained similar findings. They revealed that treatment of cancer cell lines by DOX loaded NPs evidently attenuated PARP-1 levels causing cell death in DOX resistant cancer cell lines. In 2017, Siddharth et al. have concluded that PARP-1 is an important substrate of apoptosis, whose cleavage is an important hallmark of apoptosis. In the same context, Huang et al. (2018) revealed the ability of surfactin loaded NPs to overcome MDR in DOX resistant breast cancer cells.

It worth noting that most studies worked on blocking MDR either by inhibitors or through RNA interference. However, one of the side effects from blocking efflux proteins of cancer cells was to cause serious pathological damage to some normal cells, and the vectors used in RNA interference showed the obvious disadvantage due to low efficiency and high toxicity (Robey et al., 2018). This why we did not use any MDR inhibitors in the current work. Nevertheless, DOX/MSNs exerted its anticancer effect successfully on OSCC cell line without development of drug resistance.

To sum up, our results revealed that DOX/MSNs succeeded to reduce percentage of viable cells and alter cell morphology of OSCC cell line. Moreover, it efficiently upregulated caspase-3 expression and reduced PARP-1 levels. Thus, the current work introduces DOX/MSNs as a possible efficient chemotherapeutic drug that exerts potent anticancer effect for treatment of OSCC. The superior results of DOX/MSNs over DOX indicate that loading the drug to NPs overcame the limitations of the commonly used Dox with possibly less toxicity and unfavorable side effects to OSCC patients.

CONCLUSION

In the view of the present results and discussion, it can be concluded that:

The use of ultra sonication for DOX loading on MSNs provided more stable drug delivery system with considerable loading capacity and encapsulation efficiency.Both DOX and DOX/MSNs had potent anticancer effect, which induced morphological changes in HNO-97 cell line. They both also had cytotoxic effect on HNO-97 cell line, which decreased cell viability percentage. In addition, they induced apoptosis and elevated the level of caspase-3. However, DOX/MSNs was able to overcome MDR in HNO-97 cell line by reducing expression of PARP1 and showed superior results and overcame all limitations of DOX alone so it could be used as a powerful drug for treatment of OSCC.

RECOMMENDATIONS

DOX/MSNs should be examined through clinical trials to explore its action on humans.Further studies are needed to unravel mechanism of action of PARP-1.More research work should be done to overcome MDR to improve drug efficiency

REFERENCES

1. Chen, X. J., Zhang, X. Q., Liu, Q., Zhang, J., & Zhou, G. (2018): Nanotechnology: A promising method for oral cancer detection and diagnosis. *Journal of Nanobiotechnology*, *16*(1), 1–17.
2. Du, L., Ma, S., Wen, X., Chai, J., & Zhou, D. (2017): Oral squamous cell carcinoma cells are resistant to doxorubicin through upregulation of miR-221. *Molecular Medicine Reports*, *16*(3), 2659–2667.
3. Fang, X., Wang, H., Han, D., Xie, E., Yang, X., Wei, J., Gu, S., Gao, F., Zhu, N., Yin, X., Cheng, Q., Zhang, P., Dai, W., Chen, J., Yang, F., Yang, H. T., Linkermann, A., Gu, W., Min, J., & Wang, F. (2019): Ferroptosis as a target for protection against cardiomyopathy. *Proceedings of the National Academy of Sciences of the United States of America*, *116*(7), 2672–2680.
4. Geng, H., Zhao, Y., Liu, J., Cui, Y., Wang, Y., Zhao, Q., & Wang, S. (2016): Hollow mesoporous silica as a high drug-loading carrier for regulation insoluble drug release. *International journal of pharmaceutics*, 510(1), 184-194
5. Huang, W., Lang, Y., Hakeem, A., Lei, Y., Gan, L., & Yang, X. (2018): Surfactin-based nanoparticles loaded with doxorubicin to overcome multidrug resistance in cancers. *International journal of nanomedicine*, 13, 1723-1736.
6. Ibiyeye, Kehinde M., Nordin, N., Ajat, M., & Zuki, Abu Bakar Z. (2019): Ultrastructural Changes and Antitumor Effects of Doxorubicin/Thymoquinone-Loaded CaCO(3) Nanoparticles on Breast Cancer Cell Line. *Frontiers in oncology*, 9, 599.
7. Kim, C., Castro-Aceituno, V., Abbai, R., Lee, A., Simu, Shakina Y., Han, Y., Hurh, J., Kim, Yeon-J., &Yang, Deok C. (2018): Caspase-3/MAPK pathways as main regulators of the apoptotic effect of the phyto-mediated synthesized silver nanoparticle from dried stem of Eleutherococcus senticosus in human cancer cells. *Biomedicine & pharmacotherapy*, 99, 128-133.
8. Kossatz, A. S., Pirovano, G., Demétrio, P., França, D. S., Arianna, L., Brand, C., Shah, V., Ramanajinappa, R. D., & Hedne, N. (2019): PARP1 as a biomarker for early detection and intraoperative tumor delineation in epithelial cancers. *first-in-human results*. 1–60.
9. Kossatz, A., Weber, W., Reiner., T. (2016): Optical imaging of PARP1 in response to radiation in oral squamous cell carcinoma. *PLOS ONE*, 11(1), 10-16
10. Liu, H., Zhang, Z., Chi, X., Zhao, Z., Huang, D., Jin, J., & Gao, J. (2016): Arsenite-loaded nanoparticles inhibit PARP-1 to overcome multidrug resistance in hepatocellular carcinoma cells. *Scientific Reports*, 6(8), 31009.
11. Robey, R. W., Pluchino, K. M., Hall, M. D., Fojo, A. T., Bates, S. E., & Gottesman, M. M. (2018). Revisiting the role of ABC transporters in multidrug-resistant cancer. *Nature reviews. Cancer*, *18*(7), 452–464.
12. Siddharth, S., Nayak, A., Nayak, D., Bindhani, K., & Kundu, N. (2017): Chitosan-Dextran sulfate coated doxorubicin loaded PLGA-PVA-nanoparticles caused apoptosis in doxorubicin resistance breast cancer cells through induction of DNA damage. Scientific reports, 7, 1, 2143.

12. Smolensky, D., Rathore, K., Bourn, J., & Cekanova, M. (2017): Inhibition of the PI3K/AKT Pathway Sensitizes Oral Squamous Cell Carcinoma Cells to Anthracycline-Based Chemotherapy In Vitro. *Journal of cellular biochemistry*, 118(9), 2615-2624
13. Tevatia, S., Rath, M., Rath, R. (2016): Nanotechnology: The Beginning of New Era. *International Journal of Enhanced Research in Medicines & Dental Care ISSN*, 7(3), 2349-1590.
14. Ye, Q., Liu, K., Shen, Q., Li, Q., Hao, J., Han, F., & Jiang, R. W. (2019): Reversal of multidrug resistance in cancer by multi-functional flavonoids. *Frontiers in Oncology*, *9*(6), 1–16.
15. Zhao, W., Cui, Y., Liu, L., Ma, X., Qi, X., Wang, Y., Liu, Z., Ma, S., Liu, J., & Wu, J. (2020): METTL3 Facilitates Oral Squamous Cell Carcinoma Tumorigenesis by Enhancing c-Myc Stability via YTHDF1-Mediated m6A Modification. *Molecular Therapy - Nucleic Acids*, *20*(12), 1–12.